Letter

Collisionless drag for a one-dimensional two-component Bose-Hubbard model

Daniele Contessi [1], Donato Romito [2,3], Matteo Rizzi [4,5] and Alessio Recati [2,1]

[1] *Dipartimento di Fisica, Università di Trento, 38123 Povo, Italy*

[2] *INO-CNR BEC Center, 38123 Povo, Italy*

[3] *Mathematical Sciences, University of Southampton, Highfield, Southampton SO17 1BJ, United Kingdom*

[4] *Forschungszentrum Jülich, Institute of Quantum Control, Peter Grünberg Institut (PGI-8), 52425 Jülich, Germany*

[5] *Institute for Theoretical Physics, University of Cologne, D-50937 Köln, Germany*

(Received 29 September 2020; revised 20 February 2021; accepted 31 March 2021; published 28 May 2021)

We theoretically investigate the elusive Andreev-Bashkin collisionless drag for a two-component one-dimensional Bose-Hubbard model on a ring. By means of tensor network algorithms, we calculate the superfluid stiffness matrix as a function of intra- and interspecies interactions and of the lattice filling. We then focus on the most promising region close to the so-called pair-superfluid phase, where we observe that the drag can become comparable with the total superfluid density. We elucidate the importance of the drag in determining the long-range behavior of the correlation functions and the spin speed of sound. In this way, we are able to provide an expression for the spin Luttinger parameter K_S in terms of drag and the spin susceptibility. Our results are promising in view of implementing the system by using ultracold Bose mixtures trapped in deep optical lattices, where the size of the sample is of the same order of the number of particles we simulate. Importantly, the mesoscopicity of the system, far from being detrimental, appears to favor a large drag, avoiding the Berezinskii-Kosterlitz-Thouless jump at the transition to the pair-superfluid phase which would reduce the region where a large drag can be observed.

DOI: 10.1103/PhysRevResearch.3.L022017

I. INTRODUCTION

The dynamics of multicomponent superfluids, ranging from neutron stars [1] to superconducting layers [2], is supposed to be crucially influenced by an intercomponent dissipationless drag. Such an entrainment was first discussed by Andreev and Bashkin in 1975 to describe the three-fluid hydrodynamics of a mixture of ^{3}He and ^{4}He superfluids [3]. In the previous works, the constitutive relations for the superfluid momenta were assumed to involve the transport of particles of one kind only [4–7]. Andreev and Bashkin instead introduced a superfluid stiffness matrix $n^{(s)}_{\alpha\beta}$, whose off-diagonal elements make it possible that a velocity v_β in one component generates a (super)current j_α in the other component, even without collisions:

$$j_\alpha = \sum_\beta n^{(s)}_{\alpha\beta} v_\beta. \tag{1}$$

Although the Andreev-Bashkin (AB) effect should be generic for multicomponent systems, it has never been directly observed (e.g., in helium, due to the very low miscibility of the two isotopes) and its dependence on the microscopic parameters has been obtained only for a few cases.

The high degree of control reached in manipulating ultracold multicomponent Bose gases has sparked the hope of having a platform for a detailed experimental study of the collisionless drag. However, a sizable entrainment requires relatively large quantum fluctuation beyond the mean-field equation of state. In the most standard configurations, i.e., three-dimensional gases [8,9], increasing quantum correlations amounts to increasing the interactions. This is technically feasible, but only partially viable since strong interactions lead to large three-body losses, very much reducing the lifetime of the gas. Fortunately, other routes are available to increase the role of quantum correlations, while keeping the system stable.

Very recently, configurations with reduced dimensionality have been proposed: in particular, in [10] it has been shown that when approaching the molecular phase in a double-layer dipolar gas system, the drag can become increasingly large. In [11], one-dimensional mixtures close to the so-called Tonks-Girardeau regime have been shown to exhibit a large entrainment.

Another possibility is to consider Hubbard-like models, by putting cold atoms in deep optical lattices. In this way, it is possible not only to realize strongly interacting superfluids with reduced three-body losses, but also to study new phases that do not appear in continuous systems. An analysis of the AB effect in a two-component single-band two-dimensional Bose-Hubbard model can be found in [12], where the effect of the proximity to the Mott insulating phase is discussed in detail.

In the present work, we give a detailed account of the AB drag in two-component Bose-Hubbard model on a one-dimensional ring. The reason is manyfold. The ring geometry is very convenient to study supercurrent related phenomena,

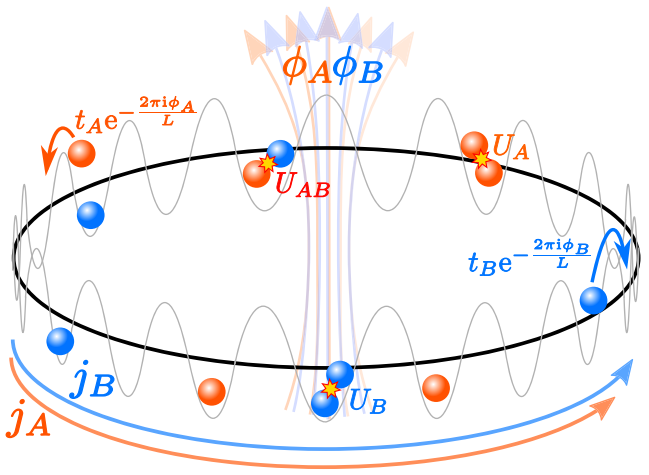

FIG. 1. Sketch of the two-component Bose-Hubbard ring with hopping parameters $\tilde{t}_\alpha = t_\alpha e^{-i2\pi\phi_\alpha/L}$, on-site intraspecies interactions U_α, and interspecies interaction U_{AB}. The two fluxes ϕ_α pierce the ring and give rise to bosonic currents j_α in the ground state.

both theoretically and experimentally [13]. The presence of the lattice allows us to have a finite range of parameters in the attractive regime where the two-superfluid state is stable and the drag can be strongly enhanced [10,12]. Moreover, differently from all the above-mentioned works based on quantum Monte Carlo (QMC) techniques, here we employ a tensor network approach, thus paving the way to study time-dependent phenomena.

We show how finite-size effects might actually increase the visibility of the collisionless drag, by circumventing the sudden jump that characterizes the phase transition to a pair-superfluid phase in the thermodynamic limit. This is particularly relevant for typical one-dimensional (1D) cold-atomic setups, where the particle number is comparable to our numerical simulations. In this respect, hyperfine state mixtures of $^{(39)41}$K atoms, or $^{4}1$K-$^{8}7$Rb mixtures (e.g., [14–18]), whose interspecies interaction can be tuned by exploiting Feshbach resonances, seem very promising to achieve the regimes where the elusive AB effect can finally be observed.

Furthermore, after determining the strength of the AB effect in various regimes, we use our microscopic approach to determine the susceptibility of the system and the relevant correlation function to extract the Luttinger parameter K_S. We show that the latter satisfies a general hydrodynamic relation with the collisionless drag, a relation which is rooted in the fact that the f-sum rule for the spin channel is not exhausted by single-phonon excitations (see [19] and the Supplemental Material of [11]). In particular, our results show how a perturbative Luttinger liquid description of the Bose-Bose Hubbard model must include an intervelocity interaction.

II. MODEL

As sketched in Fig. 1, we consider a two-species Bose-Hubbard Hamiltonian, $H = H_A + H_B + H_{AB}$, on a ring with L sites,

$$H_\alpha = \sum_{x=1}^{L}\left[-(\tilde{t}_\alpha b^\dagger_{x+1,\alpha} b_{x,\alpha} + \text{H.c.}) + \frac{U_\alpha}{2} n_{x,\alpha}(n_{x,\alpha}-1)\right],$$

$$H_{AB} = U_{AB}\sum_{x=1}^{L} n_{x,A} n_{x,B}, \tag{2}$$

where $b^\dagger_{x,\alpha}(b_{x,\alpha})$ is the bosonic creation (annihilation) operator and $n_{x,\alpha} = b^\dagger_{x,\alpha} b_{x,\alpha}$ is the number operator at site x for the species $\alpha \in \{A, B\}$. Physically, the two species can be two hyperfine levels of atoms, two band indices, or two different atomic elements or isotopes. The single-species Hamiltonian H_α accounts for the hopping between neighboring sites, with $\tilde{t}_\alpha = t_\alpha e^{-i2\pi\phi_\alpha/L}$ and $t_\alpha, \phi_\alpha \in \mathbb{R}^+$, and for the on-site repulsion characterized by the parameter $U_\alpha > 0$. The fluxes ϕ_α piercing the ring are introduced in order to compute the superfluid currents and densities [see Eqs. (4)–(6)] and are equivalent to twisted periodic boundary conditions (PBCs) [20]. The Hamiltonian H_{AB} describes the interspecies on-site interaction—responsible for the collisionless drag phenomenon—with strength U_{AB}.

We limit ourselves to a zero-temperature, $\mathbb{Z}_2$ symmetric mixture: $t_\alpha = t$, $U_\alpha = U$, and filling $\nu_\alpha \equiv N_\alpha/L = \nu/2$, in terms of the number of atoms, N_α. The phase diagram of the 1D model is very rich and has not yet been determined with the same accuracy as in higher dimensions [21,22]: to our knowledge, the most complete analysis can be found in [23]. It is beyond the scope of the present work to bridge this gap and the full phase diagram will be reported elsewhere [24]. For the purpose of the present study, we are interested in only two of the possible phases: the two-superfluid (2SF) phase and the pair-superfluid (PSF) phase. The 2SF phase is characterized by both components A and B being superfluid. The low-energy spectrum consists of two gapless linear (Goldstone) modes corresponding to a density (in-phase) and a spin (out-of-phase) mode. In the PSF phase, the two components are paired and the spin channel acquires a gap [25]. One of our goals here is to determine the superfluid density matrix in the 2SF phase while approaching the PSF, where the collisionless drag should saturate to its maximum value [10,12].

We resort to a matrix product states (MPS) ansatz to deal with the full many-body problem. The model (2) is indeed not exactly solvable and our numerical treatment is an almost unbiased approach to it. We overcome the difficulties related to PBCs by employing a loop-free geometry of the tensor network and shifting the topology of the lattice into the matrix product operator (MPO) representation of the Hamiltonian. The idea consists essentially in introducing nearest-neighbor couplings along a snakelike enumeration of the physical sites (see the Supplemental Material [26]). In this way, we can reliably compute the relevant quantities for systems up to $L = 96$ sites, achieving expectation values (e.g., of densities and currents) homogeneous up to 0.3% along the ring.

III. SUPERFLUID DENSITIES AND COLLISIONLESS DRAG

In order to determine the superfluid density matrix, we need to compute the currents on the ring. As usual, the

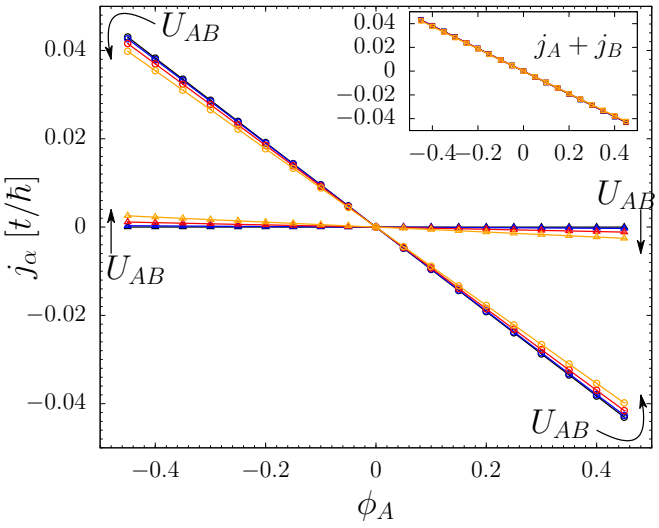

FIG. 2. The superfluid currents j_A and j_B in the presence of ϕ_A only for a $L = 32$ system. The four sets of curves (from dark to light color) correspond to $U_{AB}/U = 0.0, 0.25, 0.5, 0.75$, with $U/t = 2$ at half filling. The drag density $n^{(s)}_{AB}$ is proportional to the slope of the j_B curve in the limit of $\phi_A \to 0$. The inset demonstrates the global momentum conservation because of the constant value of the total current for all values of U_{AB}.

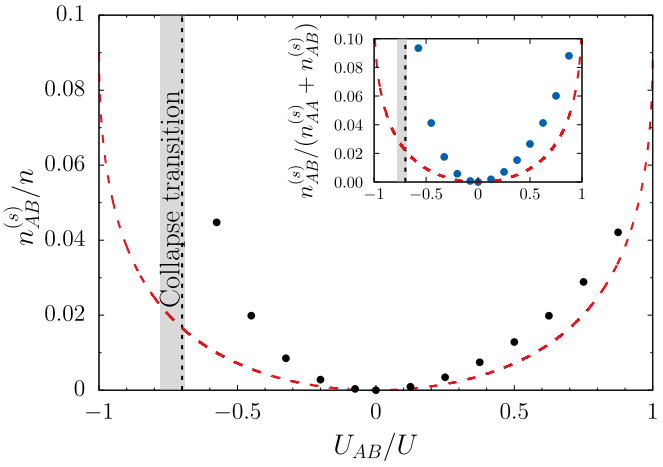

FIG. 3. Superfluid drag in terms of the total density (main panel) and of the total superfluid density (inset). The red dashed line indicates the theoretical prediction via Bogoliubov approximation [19]. The relevant pairing correlations are responsible for the nonsymmetric trend exhibited by the attractive regime ($U_{AB} < 0$).

definition of the current is properly obtained through the (discrete) continuity equation,

$$\frac{\partial\langle\hat{n}_{x,\alpha}(t)\rangle}{\partial t} = \frac{1}{i\hbar}\langle[\hat{n}_{x,\alpha}, \hat{H}]\rangle = \frac{2\tilde{t}}{\hbar}(\mathrm{Im}\langle b^\dagger_{x+1,\alpha} b_{x,\alpha}\rangle - \mathrm{Im}\langle b^\dagger_{x,\alpha} b_{x-1,\alpha}\rangle). \quad (3)$$

Thus, one can calculate the currents using the expression

$$j_\alpha = \frac{2\tilde{t}}{\hbar}\,\mathrm{Im}\langle b^\dagger_{x+1,\alpha} b_{x,\alpha}\rangle = \frac{1}{2\pi\hbar}\frac{\partial E}{\partial\phi_\alpha}, \quad (4)$$

where the last equality has been obtained by applying the Hellmann-Feynman theorem. By linearizing the currents for small fluxes and using the relation

$$v_\beta = \frac{\hbar}{m^*}\frac{2\pi\phi_\beta}{L}, \quad (5)$$

with $m^* = \hbar^2/2t$ the "band mass," we can compute the AB [3] superfluid density matrix $n^{(s)}_{\alpha\beta}$ of Eq. (1) as

$$n^{(s)}_{\alpha\beta} = \lim_{\phi_\alpha,\phi_\beta\to 0}\frac{Lm^*}{2\pi\hbar}\frac{\partial j_\alpha}{\partial\phi_\beta} = \lim_{\phi_\alpha,\phi_\beta\to 0}\frac{Lm^*}{(2\pi\hbar)^2}\frac{\partial^2 E}{\partial\phi_\alpha\partial\phi_\beta}. \quad (6)$$

It is important to notice that within tensor network methods, the total energy and current densities, computed from short-range correlations, are among the most reliable quantities to be extracted.

In Fig. 2, we illustrate the effect of the AB drag on the currents: in the presence of ϕ_A only, the current j_B is constantly zero in the absence of interspecies interaction, $U_{AB} = 0$, while it increases monotonically as U_{AB} increases. The drag density $n^{(s)}_{AB}$ is proportional to the slope of the j_B curve in the limit of $\phi_A \to 0$. The plot highlights the smallness of the drag effect at a generic point in parameter space—here, the filling is $\nu = 0.5$ with $U/t = 2$ and $L = 32$. For completeness, in the inset of Fig. 2, we report the total current and we confirm that the result $j_A + j_B = 2\pi\nu\phi_A/L$ is independent of the interaction.

A. Superfluid drag at half filling

In Fig. 3, we report the results for the drag density $n^{(s)}_{AB} = n^{(s)}_{BA}$ as a function of the interspecies interaction U_{AB}/t for half total filling $\nu = 0.5$ and $U/t = 2$. In this regime, as expected from previous analysis [23], the mixture is always in the 2SF phase until it undergoes either phase separation or collapse. The location of the phase transitions is strongly dependent on the parameters of the configuration. In our case, the collapse occurs beyond the black dashed line in the shaded region.

For comparison, the Bogoliubov prediction for the entrainment is also reported. Using the method developed in Ref. [19], the Bogoliubov approach leads to the simple expression for the drag,

$$n^{(s)}_{AB} \simeq \frac{t}{4L}\sum_k \frac{(\Omega_{d,k} - \Omega_{s,k})^2 k^2}{(\Omega_{d,k} + \Omega_{s,k})\Omega_{s,k}\Omega_{d,k}}\left[\frac{\sin(k)}{k}\right]^2, \quad (7)$$

with $\Omega_{d(s),k} = \sqrt{\epsilon(k)[\epsilon(k) + 2U\nu \pm 2U_{AB}\nu]}$ the excitation energies of the density (spin) channel and $\epsilon(k) = 4t\sin^2(k/2)$ the single-particle dispersion relation. The sum in (7) is done on the wave vectors in the first Brillouin zone, $k = 2\pi/L \cdot n$, with $n = 0, \ldots, (L-1)$. The Bogoliubov approach turns out to be not very reliable, except for very small interspecies interaction [27].

More importantly while Eq. (7) predicts a symmetric behavior for $U_{AB} \to -U_{AB}$, the data display an evident asymmetry between the two regimes concerning both the location of the transitions and the slope of the drag increase as a function of the interaction strength. In particular, the attractive mixture experiences a much steeper growth of the drag. This substantial increase can be ascribed to pairing correlations—

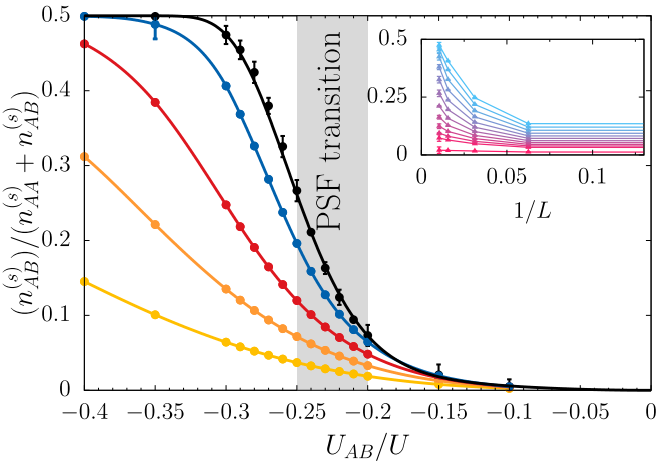

FIG. 4. Normalized drag with respect to the total superfluid density for different system sizes, as a function of U_{AB} for a system with $U = 10t$ and $\nu = 1$. From bottom to top (from light to dark shades), $L = 8, 16, 32, 64, 96$, with corresponding bond dimensions $\chi = 100, 300, 600, 700, 800$. Points are data (with error bars explained in the Supplemental Material [26]); lines are an artistic guide to the eye. The thermodynamic limit should exhibit a saturation to $(n_{AB}^{(s)})/(n_{AA}^{(s)}+n_{AB}^{(s)}) = 0.5$ in the PSF region. In the inset, the same points of the main plot are represented as a function of the inverse of the system's size L^{-1} for different values of $-0.30 \leqslant U_{AB}/U \leqslant -0.15$, from top to bottom.

relevant in 1D for any value $U_{AB} < 0$—which are not captured by the Bogoliubov approach.

B. Superfluid drag approaching the PSF phase

In analogy with the QMC results in the 2D case [10,12], we expect that the asymmetry between the attractive and repulsive regimes is strongly emphasized in the regime where a single superfluid of dimers can be reached for $U_{AB} < 0$ (PSF phase). Indeed, in the latter case, the flow of one component is accompanied by the flow of the other, i.e., $n_{AB}^{(s)} = n_{AA}^{(s)}$. The drag $n_{AB}^{(s)}$ becomes a quarter of the total superfluid density, $n^{(s)} = n_{AA}^{(s)} + n_{BB}^{(s)} + 2n_{AB}^{(s)}$, and hence saturates to its maximum possible value and simultaneously ceases to be interpreted as a drag coefficient. Before the saturation, the magnitude of the drag rapidly increases, making the approach to the PSF transition a very suitable region for its measurement. The results for different system sizes are reported in Fig. 4, where $U/t = 10$ and $\nu = 1$ are chosen such that the system can undergo the transition (see, also, [23]). In the inset, we report the behavior of the normalized drag as a function of L^{-1} for different values of the interaction. We estimate that the SF-to-PSF transition should occur in the thermodynamic limit for $U_{AB}/U \in [-0.25, -0.2]$ (shaded region in the main panel). In such a limit—belonging to the transition to the Berezinskii-Kosterlitz-Thouless universality class [23]—the saturation should happen as a sudden jump of the spin-superfluid density, $n_{AA}^{(s)} - n_{AB}^{(s)}$, from a finite value to zero. We stress, however, that mesoscopic samples such as the ones accessible in cold-atomic setups will display no jump, but rather a sizable value of $n_{AB}^{(s)}$, thus making the AB collisionless drag finally observable.

IV. COLLISIONLESS DRAG AND LUTTINGER LIQUID PARAMETERS

After having extracted the strength of collisionless drag and found the regime where its presence is not negligible, we study its effect in determining the behavior of some correlation functions and its relationship with the Luttinger liquid (quantum hydrodynamic) low-energy description of the two-species Bose-Hubbard model.

Indeed, in the 2SF phase, the low-energy theory for our system corresponds to the Hamiltonian of two coupled Luttinger liquids [28]. The Hamiltonian can be diagonalized by introducing the density (D) and spin/polarization (S) channels,

$$H_\mu = \frac{1}{2\pi}\int \left[c_\mu K_\mu (\partial_x \phi_\mu)^2 + \frac{c_\mu}{K_\mu}(\partial_x \theta_\mu)^2\right] dx, \tag{8}$$

where $\phi_{D(S)} = (\phi_A \pm \phi_B)/\sqrt{2}$ and $\theta_{D(S)} = (\theta_A \pm \theta_B)/\sqrt{2}$ are the bosonic fields related to the fluctuations of the phase and the amplitude of the total density (spin) of the two coupled superfluids [29]. The speeds of sound, $c_{D(S)}$ and $K_{D(S)}$, are the so-called Luttinger parameters. There is an additional nonlinear coupling between the densities of the two Luttinger liquids, which can be perturbatively accounted for by a term proportional to $U_{AB}\cos(2\sqrt{2}\theta_S)$. This term is irrelevant in the 2SF phase and relevant in the PSF phase. As long as the Hamiltonian given by Eq. (8) holds, an algebraic decay characterizes the correlation functions (also known as quasi-long-range order) [28],

$$\begin{aligned} G_\alpha(x) &= \langle b^\dagger_{i+x,\alpha} b_{i,\alpha}\rangle \propto |d|^{-\frac{1}{4K_D}-\frac{1}{4K_S}}, \\ R_D(x) &= \langle b^\dagger_{i+x,A} b^\dagger_{i+x,B} b_{i,B} b_{i,A}\rangle \propto |d|^{-\frac{1}{K_D}}, \\ R_S(x) &= \langle b^\dagger_{i+x,A} b_{i+x,B} b^\dagger_{i,B} b_{i,A}\rangle \propto |d|^{-\frac{1}{K_S}}. \end{aligned} \tag{9}$$

Here we expressed the algebraic decay in terms of the natural measure of the distances between sites on a ring geometry, i.e., the *chord* function [30],

$$d(x/L) = \frac{L}{\pi}\sin\left(\frac{\pi x}{L}\right), \tag{10}$$

where L is the number of sites and $x \in \mathbb{N}$ is the linear distance between the sites. For very large rings, the expression further simplifies according to the substitution $d \to x$. The relations in (9) can be easily checked by using the leading term in the long-wavelength field representation $b_{j,\alpha} \propto \exp(i\phi_\alpha)$ [31].

The single-body correlations G_α have a mixed density/spin character, consistent with the fact that the imaginary part of their nearest-neighbor value gives back the species current j_α. The two contributions can instead be isolated with the help of two-body correlations: R_D concerns the superfluid character of pairs of $A-B$ particles and therefore the density channel, while R_S relates to particle-hole pairs and therefore the spin channel [12,23].

Away from commensurate effects, possibly leading to a Mott insulator, the density channel is always superfluid, i.e., R_D scales algebraically. A change in R_S and G_α from algebraic to exponential decay—or, equivalently, a drop of K_S to 0—happens instead when entering the PSF phase, due to the opening of a gap in the spin channel. This is illustrated

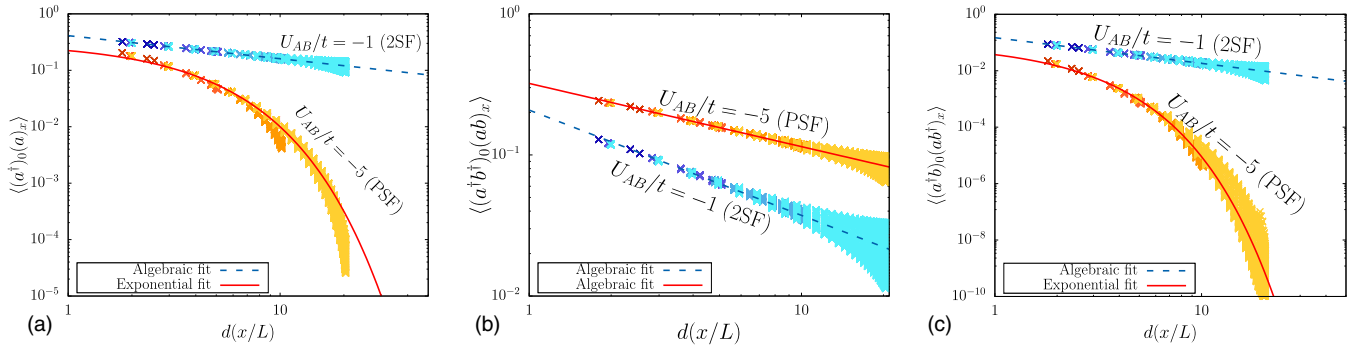

FIG. 5. The correlation functions of Eq. (9) [(a) G_α, (b) R_D, and (c) R_S] as a function of the conformal distance for a unitary total filling system $\nu = 1$, $t = 1$, and $U = 10$. The orange points concern a regime in which the system is in a PSF phase, while the blue ones concern the 2SF phase, and we represent, with a color gradient from dark to light, different system sizes from $L = 8$ to $L = 64$. The dashed lines are exponential and algebraic fits, depending on the expected behavior of the functions for $U_{AB}/U = -0.1$, and the solid lines are for $U_{AB}/U = -0.5$.

in Fig. 5, where the correlations measured for different system sizes ($L = 8, 16, 32, 64, 96$) are reported for two sample parameter values deep in the 2SF (blue) and PSF (orange) phases.

The Luttinger parameters satisfy the relation [28]

$$K_S = \pi\hbar\chi c_S/2, \tag{11}$$

where $\chi = [\partial^2 e/\partial(\nu_A - \nu_B)^2]^{-1}$ is the spin susceptibility, with e the energy density (the same goes for the density channel with the compressibility rather than the susceptibility).

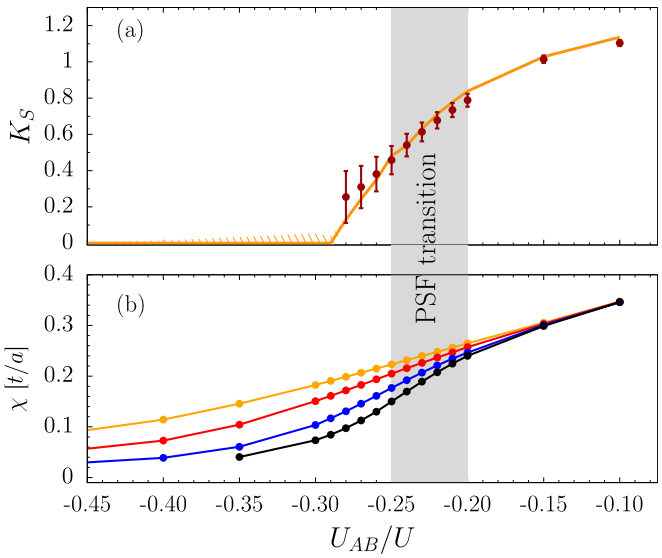

FIG. 6. (a) Luttinger parameter K_S for the spin channel, as obtained from the hydrodynamic relation in Eq. (13) (solid line with error shadow) and from the correlation functions, given by Eq. (9) (points with error bars). Points are reported until the algebraic fit makes sense: the shaded region indicates where deviations become sizable (for more details, see the Supplemental Material [26]). In the PSF, the parameter K_S must go to zero. (b) The behavior of the susceptibility as a function of the interaction, as estimated from various system sizes (color code as in Fig. 4, except for $L = 8$ which is omitted).

On the other hand, a hydrodynamic approach based on the energy functional including the collisionless drag [3,10] provides the following relation between the spin speed of sound and the superfluid densities [32]:

$$c_S^2 = 2\frac{n_{AA}^{(s)} - n_{AB}^{(s)}}{m^*\chi}. \tag{12}$$

By direct comparison, the following also holds:

$$K_S = \sqrt{\frac{\pi^2\hbar^2\left(n_{AA}^{(s)} - n_{AB}^{(s)}\right)\chi}{2m^*}}. \tag{13}$$

The drag thus appears in the constitutive relations of the Luttinger parameters. This fact, often overlooked in the literature [23,33–37], is crucial in obtaining consistent results in the perturbative approach of Luttinger liquids. Therefore, in writing the two-species Luttinger Hamiltonian, a term proportional to $n_{AB}^{(s)}\partial_x\phi_A\partial_x\phi_B$ must be included. The latter term should indeed be generated under the renormalization group flow obtained by means of the operator product expansion as it has been studied for the Josephson tunneling between superfluids (see, e.g., [38] and reference therein). In Fig. 6, we report the values of K_S obtained by hydrodynamics [Eq. (13)] and by the long-range behavior of the correlation functions [Eq. (9)].

The latter, however, ceases to be algebraic and becomes exponential once the system enters into the PSF phase [23]: we quantify this change by measuring the deviation from a pure algebraic behavior in log-log scale (see the Supplemental Material [26] for a detailed discussion). The region where the deviation becomes appreciable is in agreement with the region predicted from the drag saturation (Fig. 4). Before the fluctuations region, the two estimates for K_S give consistent results.

For the sake of comparison with mesoscopic experiments accessible with ultracold gases in optical lattices, we also report, in Fig. 6(b), the estimated spin susceptibility for different system sizes.

V. CONCLUSIONS

In conclusion, we provide a numerical estimation of the AB superfluid drag via a tensor network approach for a 1D Bose mixture on a ring lattice. The drag is enhanced for attractive interactions due to the relevance of pairing correlations in 1D systems. In particular, close to the 2SF-PSF transition, the entrainment can become of the same order of the full superfluid density, which makes this regime more suitable for an experimental measure. Differently from the Mott-superfluid case for a single species [38,39], the thermodynamic estimate of the PSF transition proves to be challenging from a numerical point of view due to the slow convergence to the thermodynamic limit for the spin channel [11]. We stress again that our results are relevant for an ultracold-gas experiment where tens to a few hundreds of atoms are considered, where the drag could be extracted by measuring the susceptibility [40] and the spin speed of sound [41].

Moreover, our analysis suggests that the inclusion of the drag has fundamental implications in the understanding of any hydrodynamic Luttinger liquid approach to the two-species Bose-Hubbard model. In particular, we show that AB hydrodynamics provides a reliable expression for the Luttinger parameters of the spin channel in terms of the superfluid densities and the susceptibility of the system.

Note added. Recently, we became aware of a density matrix renormalization group (DMRG)-QMC comparison for the study of the pairing properties of one-dimensional hard-core bosons [42]. The results show the slow convergence to the thermodynamic limit for the spin channel as in our soft-core case.

ACKNOWLEDGMENTS

We gratefully acknowledge insightful discussions with S. Giorgini, A. Haller, S. Manmana, J. Nespolo, and S. Stringari. M.R. acknowledges partial support from the Deutsche Forschung Gesellschaft (DFG) through the individual Grant No. 277810020 (RI 2345/2-1) and the CRC network TRR183 Grant No. 277101999 (unit B01), the European Union (PASQuanS, Grant No. 817482), the Alexander von Humboldt Foundation, and the kind hospitality of the BEC Center in Trento, where a great part of this study was performed. D.C. acknowledges hospitality at the Johannes Gutenberg University Mainz, where preliminary stages of this work were conducted. A.R. acknowledges financial support from the Italian MIUR under the PRIN2017 project CEnTraL, the Provincia Autonoma di Trento, and the Q@TN initiative. The MPS simulations were run on the Mogon Cluster of the Johannes Gutenberg-Universität Mainz (made available by the CSM and AHRP) and on the JURECA Cluster at the Forschungszentrum Jülich, with a code based on a flexible Abelian Symmetric Tensor Networks Library, developed in collaboration with the group of S. Montangero (Padua).

[1] J. M. Lattimer and M. Prakash, The physics of neutron stars, Science **304**, 536 (2004).

[2] Ji-Min Duan and S. Yip, Supercurrent Drag Via the Coulomb Interaction, Phys. Rev. Lett. **70**, 3647 (1993).

[3] A. Andreev and E. Bashkin, Three-velocity hydrodynamics of superfluid solutions, Zh. Eksp. Teor. Fiz. **69**, 319 (1975). [Sov. Phys. JETP **42**, 164 (1976)].

[4] I. M. Khalatnikov, Hydrodynamics of solutions of two superfluid liquids, J. Exptl. Theoret. Phys. (U.S.S.R.) **32**, 653 (1957) [Sov. Phys. JETP **5**, 542 (1957)].

[5] I. M. Khalatnikov, Hydrodynamics of solutions of two superfluid liquids, ZhETF Pis. Red. **17**, 534 (1973) [JETP Lett. **17**, 386 (1973)].

[6] Z. M. Galasiewicz, Hydrodynamics of solutions of two superfluid liquids, Phys. Lett. A **43**, 149 (1973).

[7] V. P. Mineev, Hydrodynamics of solutions of two superfluid liquids, Zh. Eksp. Teor. Fiz. **67**, 683 (1974) [Sov. Phys. JETP **40**, 338 (1974)].

[8] D. V. Fil and S. I. Shevchenko, Nondissipative drag of superflow in a two-component Bose gas, Phys. Rev. A **72**, 013616 (2005).

[9] J. Linder and A. Sudbø, Calculation of drag and superfluid velocity from the microscopic parameters and excitation energies of a two-component Bose-Einstein condensate in an optical lattice, Phys. Rev. A **79**, 063610 (2009).

[10] J. Nespolo, G. E. Astrakharchik, and A. Recati, Andreev-Bashkin effect in superfluid cold gases mixtures, New J. Phys. **19**, 125005 (2017).

[11] L. Parisi, G. E. Astrakharchik, and S. Giorgini, Spin Dynamics and Andreev-Bashkin Effect in Mixtures of One-Dimensional Bose Gases, Phys. Rev. Lett. **121**, 025302 (2018).

[12] K. Sellin and E. Babaev, Superfluid drag in the two-component Bose-Hubbard model, Phys. Rev. B **97**, 094517 (2018).

[13] W. Kohn, Theory of the insulating state, Phys. Rev. **133**, A171 (1964).

[14] G. Semeghini, G. Ferioli, L. Masi, C. Mazzinghi, L. Wolswijk, F. Minardi, M. Modugno, G. Modugno, M. Inguscio, and M. Fattori, Self-Bound Quantum Droplets of Atomic Mixtures in Free Space, Phys. Rev. Lett. **120**, 235301 (2018).

[15] G. Ferioli, G. Semeghini, L. Masi, G. Giusti, G. Modugno, M. Inguscio, A. Gallemí, A. Recati, and M. Fattori, Collisions of Self-Bound Quantum Droplets, Phys. Rev. Lett. **122**, 090401 (2019).

[16] C. R. Cabrera, L. Tanzi, J. Sanz, B. Naylor, P. Thomas, P. Cheiney, and L. Tarruell, Quantum liquid droplets in a mixture of Bose-Einstein condensates, Science **359**, 301 (2018).

[17] L. Tanzi, C. R. Cabrera, J. Sanz, P. Cheiney, M. Tomza, and L. Tarruell, Feshbach resonances in potassium Bose-Bose mixtures, Phys. Rev. A **98**, 062712 (2018).

[18] C. D'Errico, A. Burchianti, M. Prevedelli, L. Salasnich, F. Ancilotto, M. Modugno, F. Minardi, and C. Fort, Observation of quantum droplets in a heteronuclear bosonic mixture, Phys. Rev. Res. **1**, 033155 (2019).

[19] D. Romito, C. Lobo, and A. Recati, Linear response study of collisionless spin drag, arXiv:2002.03955.

[20] A. J. Leggett, Topics in the theory of helium, Phys. Fenn. **8**, 125 (1973).

[21] A. B. Kuklov and B. V. Svistunov, Counterflow Superfluidity of Two-Species Ultracold Atoms in a Commensurate Optical Lattice, Phys. Rev. Lett. **90**, 100401 (2003).

[22] A. Kuklov, N. Prokof'ev, and B. Svistunov, Commensurate Two-Component Bosons in an Optical Lattice: Ground State Phase Diagram, Phys. Rev. Lett. **92**, 050402 (2004).

[23] A. Hu, L. Mathey, I. Danshita, E. Tiesinga, C. J. Williams, and C. W. Clark, Counterflow and paired superfluidity in one-dimensional Bose mixtures in optical lattices, Phys. Rev. A **80**, 023619 (2009).

[24] D. Contessi, A. Recati, and M. Rizzi, (unpublished).

[25] This phase is sometimes considered the bosonic counterpart of the much more relevant phenomenon of pair condensation occurring in fermionic systems.

[26] See Supplemental Material at http://link.aps.org/supplemental/10.1103/PhysRevResearch.3.L022017 for some details about the realization of periodic boundary conditions, the procedures for the numerical derivatives and the errors and the extraction of the Luttinger parameters from the correlation functions.

[27] The same occurs in a continuous one-dimensional Bose mixture with repulsive interactions [11], where the Monte Carlo results are compared with the continuous version of Eq. (7), i.e., by replacing, in Eq. (7), $t \to \hbar^2/2m$ and $\sin(k)/k \to 1$.

[28] T. Giamarchi, *Quantum Physics in One Dimension* (Oxford University Press, Oxford, 2004).

[29] In particular, the long-wavelength representation of the single-particle operators is $b_{x,\alpha} \to (n + \partial_x\theta_\alpha)^{1/2} \sum_m \exp[2\pi i m(\theta_\alpha + \pi n x)]e^{i\phi_\alpha}$; see, e.g., [23,28].

[30] M. A. Cazalilla, R. Citro, T. Giamarchi, E. Orignac, and M. Rigol, One dimensional bosons: From condensed matter systems to ultracold gases, Rev. Mod. Phys. **83**, 1405 (2011).

[31] F. D. M. Haldane, Effective harmonic-Fluid Approach to Low-Energy Properties of One-Dimensional Quantum Fluids, Phys. Rev. Lett. **47**, 1840 (1981).

[32] Let us remind the reader that in a Galilean invariant system, one has that at $T = 0$, the total superfluid density is equal to the total density, i.e., $2(n^{(s)}_{AA} + n^{(s)}_{AB}) = n$, and therefore the numerator of Eq. (12) would be fully determined by the drag [10].

[33] A. Kleine, C. Kollath, I. P. McCulloch, T. Giamarchi, and U. Schollwöck, Spin-charge separation in two-component Bose gases, Phys. Rev. A **77**, 013607 (2008).

[34] A. Kleine, C. Kollath, I. P. McCulloch, T. Giamarchi, and U. Schollwöck, Excitations in two-component Bose gases, New J. Phys. **10**, 045025 (2008).

[35] L. Mathey, I. Danshita, and C. W. Clark, Creating a supersolid in one-dimensional Bose mixtures, Phys. Rev. A **79**, 011602(R) (2009).

[36] E. Orignac, R. Citro, M. Di Dio, and S. De Palo, Vortex lattice melting in a boson ladder in an artificial gauge field, Phys. Rev. B **96**, 014518 (2017).

[37] R. Citro, S. De Palo, M. Di Dio, and E. Orignac, Quantum phase transitions of a two-leg bosonic ladder in an artificial gauge field, Phys. Rev. B **97**, 174523 (2018).

[38] L. Benfatto, C. Castellani, and T. Giamarchi, Berezinskii–Kosterlitz–Thouless transition within the sine-Gordon approach: The role of the vortex-core energy, in *40 Years of Berezinskii–Kosterlitz–Thouless Theory*, edited by J. V. José (World Scientific (Singapore), 2013), pp. 161–199.

[39] M. Gerster, M. Rizzi, F. Tschirsich, P. Silvi, R. Fazio, and S. Montangero, Superfluid density and quasi-long-range order in the one-dimensional disordered Bose-Hubbard model, New J. Phys. **18**, 015015 (2016).

[40] T. Bienaimé, E. Fava, G. Colzi, C. Mordini, S. Serafini, C. Qu, S. Stringari, G. Lamporesi, and G. Ferrari, Spin-dipole oscillation and polarizability of a binary Bose-Einstein condensate near the miscible-immiscible phase transition, Phys. Rev. A **94**, 063652 (2016).

[41] J. H. Kim, D. Hong, and Y. Shin, Observation of two sound modes in a binary superfluid gas, Phys. Rev. A **101**, 061601(R) (2020).

[42] B. Grémaud and G. G. Batrouni, Pairing and pair superfluid density in one-dimensional Hubbard models, arXiv:2006.13950.